Functional Genetic Assays of Immunometabolic Reporters

By

Emma Lieberman

A Thesis Presented in Partial Fulfillment
of the Requirements for the Degree
Master of Science

Approved April 2023 by the
Graduate Supervisory Committee:

Benjamin Bartelle, Chair
Christopher Plaisier
Madeline Andrews

ARIZONA STATE UNIVERSITY

May 2023

ABSTRACT

Characterizing and identifying neuroinflammatory states is crucial in developing treatments for neurodegenerative diseases. Microglia, the resident immune cells of the brain, regulate inflammation and play a vital role in maintaining brain health by producing cytokines, performing phagocytosis, and inducing or reducing inflammation. These functional states can be described by specific patterns of gene expression called transcriptional programs, which are determined by the activity of a set of key transcription factors that have mostly been identified. Thus, an assay for transcription factor activity could reveal the state of the microglial cells and neuroinflammation across the brain. This research developed an assay that uses a transcription factor dependent reporter to indicate which transcriptional programs are activated in the cell when exposed to different stimuli. The prototype assay quantifies nuclear factor kappa B (NF-kB) response in cultured human cells. NF-kB is a well-characterized transcription factor associated with inflammatory pathways in most cells, including microglia. The reporter construct contains an NF-kB specific responsive element that can induce fluorescence/luminescence upon activation of the transcription factor. In an iterative refinement, a dual response fluorescent reporter was developed, which uses a secondary constitutively fluorescent reporter for built-in normalization of the responsive element for microscopy studies. With further refinement, this modular system will serve as a template for less understood transcriptional enhancers allowing for rapid, low-cost assays of neuroimmune regulators and potential in vivo applications in the study of neuroinflammation.

i

TABLE OF CONTENTS

LIST OF TABLES

LIST OF FIGURES

INTRODUCTION

Neurodegenerative diseases, such as Alzheimer's and Parkinson's can cause a detrimental persistent immune response in the brain leading to long-term negative effects. Alzheimer's and Parkinson's are the leading neurodegenerative diseases in the United States (*Neurodegenerative Diseases*, 2022). Both diseases pose an economic burden on the US. Parkinson's related care totaled over $51 billion in 2017 (Yang et al., 2020), and Alzheimer's related care is precited to cost $345 billion in 2023 ("2023 Alzheimer's Disease Facts and Figures," 2023). Alzheimer's disease is characterized by loss of memory and decreased cognitive function due to loss of brain volume. This decline in health is due to the accumulation of amyloid-beta (AB) protein plaques in the brain. Parkinson's disease, which is characterized by tremors, rigidity, and occasionally dementia, is caused by the accumulation of the protein alpha-synuclein (a-syn) in the brain. (Hammond et al., 2019). While these two diseases affect patients differently, involve different proteins, and affect a wide array of neuronal cells, they both result in neurodegeneration due to prolonged neuroinflammation. Neuroinflammation is the production of inflammatory cytokines, chemokines, reactive oxygen species, and secondary messengers produced in the central nervous system primarily by microglia (DiSabato et al., 2016).

Microglia are the resident immune cells of the central nervous system and perform a variety of roles including synaptic pruning of neurons, tissue surveillance, cytokine secretion, and phagocytosis of debris and pathogens (Paolicelli et al., 2022; Salter & Stevens, 2017). They play a role in the progression of Alzheimer's and

Parkinson's by localizing to the protein accumulations and failing to phagocytose all the accumulated protein, and by releasing inflammatory cytokines that induce a prolonged inflammatory state (Hammond et al., 2019). While microglia are not the only cells causing these diseases, targeting them is beneficial because they impact a wide variety of neurodegenerative diseases, and play a role in traumatic brain injury and viral infection as well as neurodegeneration. Microglia take on many roles in the brain and understanding them thoroughly is the first step toward identifying a potential treatment for these diseases.

Microglia are the predominant immune cells of the brain and are largely responsible for neuroinflammatory responses to disease, infection, and injury (Muzio et al., 2021, Shao et al., 2022). Understanding and treating neurodegenerative diseases requires the identification and classification of the distinct microglial functional states that arise from and drive pathology. Early models of microglial function only classified M1 (pro-inflammatory) or M2 (anti-inflammatory) states (Lively & Schlichter, 2018). However, a much wider range of morphological phenotypes have been described and a spectrum of functional states are broadly acknowledged including inflammation, myelination, neurogenesis, and synapse remodeling (Paolicelli et al., 2022; Shao et al., 2022). Classifying microglia is a complex problem that must consider cell morphology, function, and cytokine production (Lier et al., 2021; Paolicelli et al., 2022). Underlying the roles of microglia are transcriptional programs triggered by neuroimmune signaling pathways. These functional programs have provided insight into microglial roles, and transcriptomic analysis is one reliable way to study cell state. Transcriptomic analysis is

used to define neurodegenerative diseases because they are difficult to classify by a single marker.

While no single gene is a reliable indicator of microglial state, recent work using transcriptomic data illuminates a method to identify features of microglial cells using a limited number of genes, using transcriptomic analysis, with further reduction to the transcription factors responsible (Cho et al., 2019). Using transcriptomic analysis methods like PCA to find covariantly expressed gene signatures or differential expression analysis to determine cluster-specific signatures offers a list of upregulated genes. Because the human genome is known and most transcriptional enhancer elements are known or predicted, the transcription factors responsible for gene expression can be predicted by looking for enrichment of their downstream targets and comparing against a Transcription Factor-target gene database using Fisher's exact test (Plaisier et al., 2016). With these tools, defining neuroimmune states based on transcription factor activation, instead of transcriptomics, could provide a rapid method of screening for microglial states. Making these rapid assays possible requires one further technology, however: a transcriptional reporter.

Reporter genes such as luciferase and GFP offer a direct readout of gene expression and have been used reliably to measure gene expression in many cell types for years (Brasier & Ron, 1992). All eukaryotic genes, whether natural or synthetic, must be driven by a promoter, which is regulated by an enhancer element. One common use of reporter genes is to mark cells using a constitutively active promoter/enhancer, often derived from a virus like SV40 or CMV. Other promoter/enhancers are conditionally

expressed by a specific cell type or in response to dynamic transcription factors. By utilizing the same enhancers conditionally expressed by a transcriptional program, or molecular pathway of interest we can create a transcriptional reporter or a direct assay of transcription factor activity. We designed our prototype transcriptional reporter around the most well-studied inflammatory promoters to take advantage of established activation paradigms and to serve as a template for less understood enhancers in future iterations.

Nuclear factor kappa B (NF-kB) is a well-known transcription factor complex that mediates inflammatory response in a wide array of cells, including microglia (Liu et al., 2017). NF-kB subunits can be activated through multiple signaling pathways (Figure 1). Two of the NF-kB subunits form a dimer and accumulate in the nucleus, where they bind a specific DNA sequence and promote transcription of the downstream genes. This specific DNA sequence, the NF-kB responsive element, has been identified and used as a reporter to measure NF-kB activation previously (Hellweg et al., 2006). NF-kB response can be induced in a variety of cells, including microglia, by different stimuli. In microglial cells, the NF-kB pathway is commonly triggered with lipopolysaccharides (LPS) (Baek et al., 2021; Lively & Schlichter, 2018). LPS binds to the Toll-like receptor 4 (TLR) inducing a well-known signaling pathway that activates NF-kB via MyD88 and/or the TRIF/TRAM pathways (Verstrepen et al., 2008; Yu et al., 2020) (Figure 1). The NF-kB pathway is not limited to only microglia. In human embryonic kidney (HEK) cells, the NF-kB pathway can be triggered with phorbol-12-myristate 13-acetate (PMA) (Hellweg et al., 2006). PMA passes through the membrane of the cell and binds to protein kinase c (PKC) which interacts with well-established signaling pathways to activate NF-kB (Lim et al., 2015; Zhang et al., 2023) (Figure 1). Because the NF-kB signaling

pathway is a well-established player in inflammatory response and the expression of the

NF-kB transcription factor can be reliably stimulated in a variety of different cell types,

we utilized it for our proof-of-concept assay.

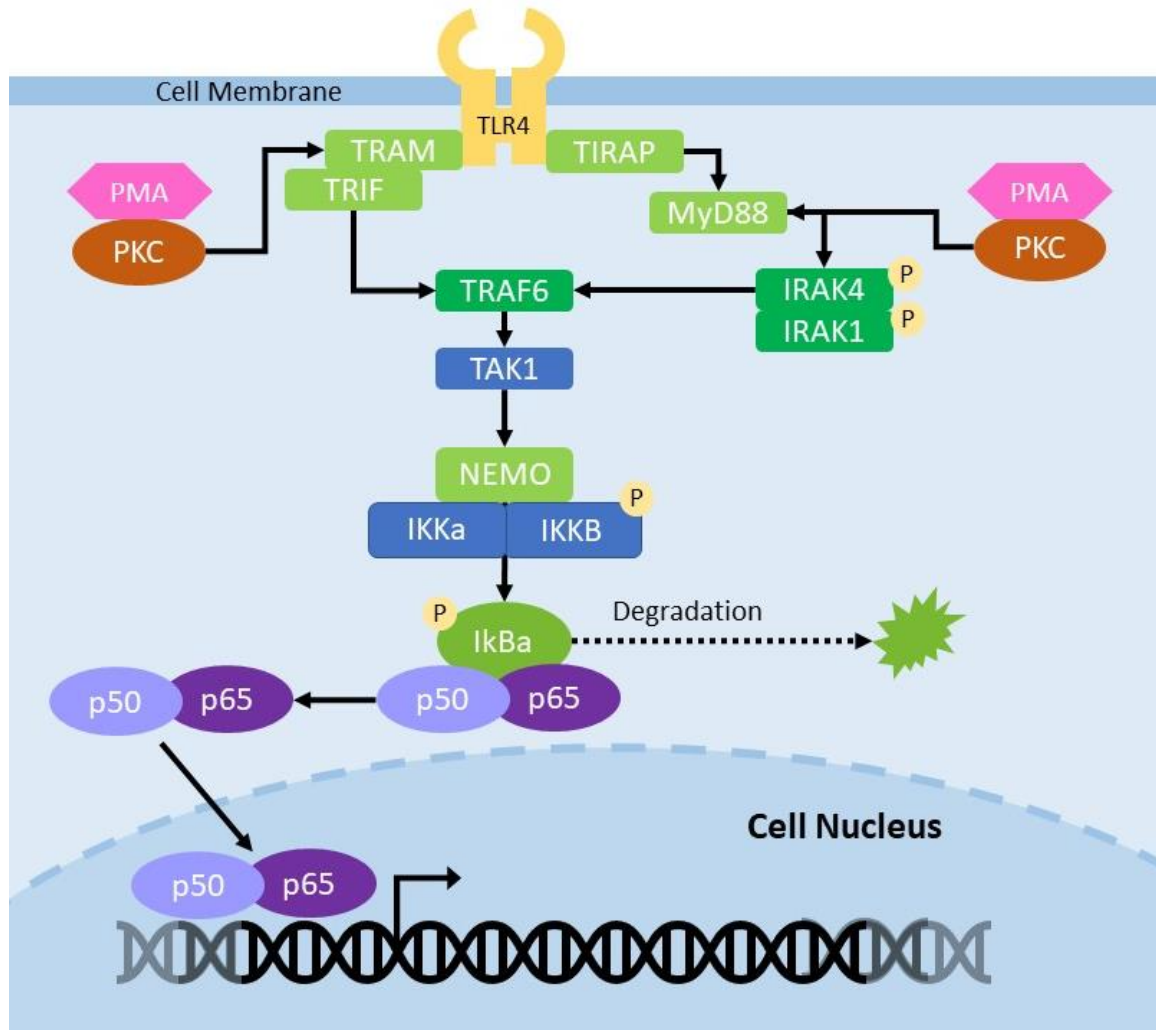**Figure 1:** Activation of the NF-kB pathway via the Toll-Like Receptor 4 (TLR) or PMA activation of Protein Kinase C (PKC). NF-kB transcription factor dimers localize to the nucleus and bind the NF-kB-specific responsive element promoting gene expression. Adapted from (Lim et al., 2015; Vallabhapurapu & Karin, 2009; Verstrepen et al., 2008; Yu et al., 2020; Zhang et al., 2023)

METHODS

Molecular Cloning

Reporter plasmids were constructed using standard molecular cloning techniques such as Gibson Assembly and Golden Gate. Gibson Assembly combines two DNA fragments that have >20 overlapping base pairs via enzymatic recombination (Gibson et al., 2009). Golden Gate Assembly utilizes type IIS restriction enzymes to enable unidirectional plasmid digestion and recombination with specific 'sticky ends' or compatible overhangs (Engler et al., 2008). Compatible overhangs were specifically designed in primers R6.3 and R6.4, and the sequences are highlighted in yellow in figures 4 and 7. The primers and g-blocks used in these cloning methods were designed in Benchling and were synthesized by Integrated DNA Technologies (IDT). Restriction enzymes XbaI, BamHI, EcoRI, and PaqCI were used to clone the constructs listed in Table 1 and shown in Figures 2-7, but not all enzymes were required for each reporter construct. Restriction enzymes, NEB-10 competent cells, and other cloning buffers and reagents were primarily acquired from New England Biolabs (NEB) or Qiagen. Successful cloning of each construct was verified via colony PCR and/or restriction digest, and sequencing by Plasmidsaurus.

Cloning 'nLuc-ON' Construct

First, we designed a constitutively active reporter, 'nLuc ON.' This construct will express the red fluorescence protein dsRed and the luminescence protein nanoLuciferase (nLuc) when transfected into mammalian cells with or without inflammatory stimulus. We expect to see high levels of dsRed and nLuc expression with or without the addition

of inflammatory drugs. It serves as a positive control for protein expression. The construct 'nLuc-ON' (Fig. 2A) was modified from the 'pLenti CMV GFP Puro' backbone engineered by (Campeau et al., 2009). It contains a constitutively active CMV enhancer/promoter upstream dsRed and nLuc. The backbone was digested with BamHI and EcoRI restriction enzymes. The insert was generated via PCR using the primers listed in Figure 2B. The responsive elements were then cloned into the backbone using standard Gibson cloning and were verified via colony PCR and restriction digest.
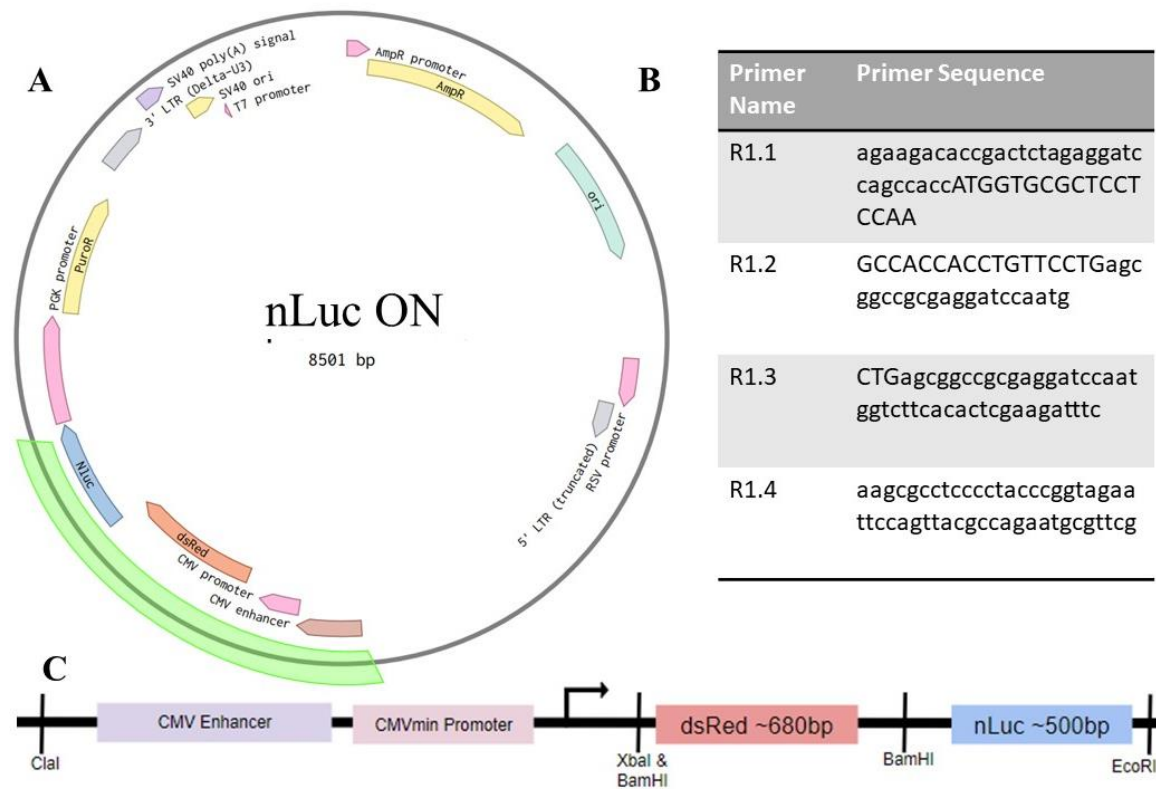

*Figure 2: Reporter Construct nLuc ON. **A.** Full reporter construct. **B.** Primers used in the construction of the reporter. **C.** Detailed view of the area highlighted in green on the vector shows the engineered region of the construct. The restriction sites, CMV enhancer/promoter, and reporters are shown. Adapted from the 'pLenti CMV GFP Puro' backbone from Campeau et al., 2009.*

Cloning 'CMVmin nLuc' Construct

To test the background noise of the CMV minimal promoter, we developed 'CMVmin nLuc'. This construct will only express minimal background fluorescence/luminescence that occurs because of the CMVmin promoter without an enhancer sequence. It serves as a negative control for background protein expression. We expect to see minimal dsRed or nLuc expression even when stimulated with inflammatory drugs. The 'CMVmin nLuc' (Fig. 3A) construct includes the addition of the mScarlet sequence in place of the CMV enhancer in between two PaqCI sites to allow for easier screening of successful cloning. The mScarlet sequence is flanked by a bacterial promoter, ribosome binding site, and terminator obtained from the iGEM registry (Kittleson, 2012; Shetty, 2003) as well as Type IIS PaqCI restriction sites (Figure 2C). This construct was cloned using the 'nLuc-ON' backbone. The backbone was digested using XbaI and ClaI, and an insert was generated by performing PCR using the primers listed in Figure 3B and the mScarlet sequence from the iGEM registry. It should be noted that the primers include the addition of the PaqCI restriction enzyme recognition site as well as specific overhangs to allow for Golden Gate cloning in the future. The CMV enhancer was excised and the mScarlet with the promoter/terminator and PaqCI Golden Gate compatible sites were inserted via Gibson cloning. The construct was verified via colony PCR and restriction digest. The addition of mScarlet under a bacterial

promoter causes the cloned bacteria with this construct to appear bright pink. This will serve as a cloning control for future design iterations.
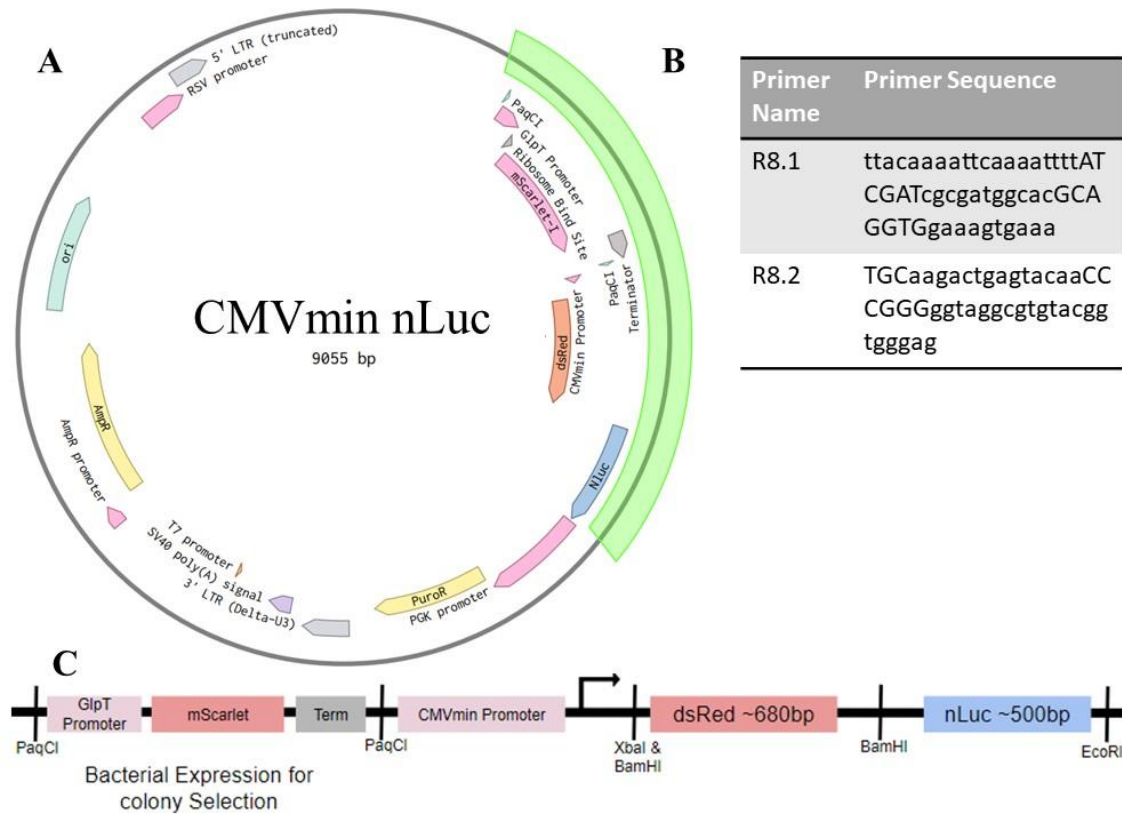
Figure 3: *Reporter construct CMVmin nLuc. **A**. Full reporter construct. **B**. Primers used in the construction of the reporter. **C**. Detailed view of the area highlighted in green on the vector shows the engineered region of the construct. This construct originated from nLuc ON and replaced the CMV enhancer with a bacterial fluorescence protein flanked by PaqCI restriction sites to enable future cloning.*

Cloning 'NF-kB nLuc' Construct

The 'NF-kB nLuc' construct is the transcription factor dependent reporter we set out to engineer. It contains the NF-kB responsive element as an enhancer sequence paired with the CMVmin promoter. We expect to see production of the reporter proteins, dsRed and nLuc, only when NF-kB is produced in the cells. The 'NF-kB nLuc' construct was cloned via Gibson assembly using the 'CMVmin nLuc' backbone. This construct replaced the mScarlet placeholder with the NF-kB responsive element from (Pomerantz et al., 2002), but kept the CMVmin promoter. The primers were designed to form an

9

annealed oligo including two NF-kB responsive elements with overhangs compatible with the PaqCI sites (Figure 4A). The NF-kB responsive element sequence was obtained from Pomerantz et al. and was verified on JASPAR (Figure 4A). The CMVmin nLuc backbone was digested with PaqCI and the annealed oligo containing the NF-kB responsive elements was inserted using Gibson cloning. The resulting reporter contains two NF-kB responsive elements upstream of the CMVmin promoter and the reporters (Figure 4C). The construct was verified by the lack of pink bacterial colonies, colony PCR, and sequencing.
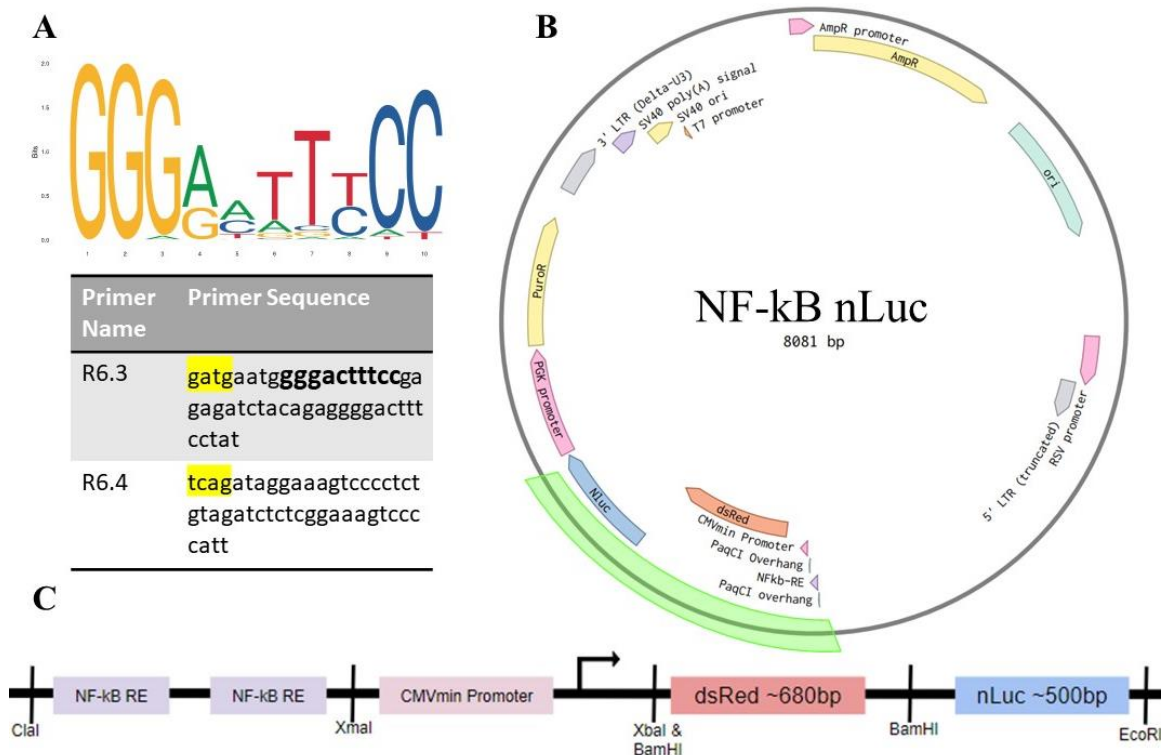

Figure 4: The NF-kB nLuc reporter. **A**. The NF-kB responsive element motif from JASPAR and the primers used to construct the NF-kB responsive region of the construct. NF-kB motif in bold and PaqCI overhangs highlighted in yellow. **B.** The completed construct. **C.** Detailed view of the engineered region of the construct that is highlighted in green.

Cloning 'NF-kB IFNB' Construct

In addition to creating a novel NF-kB reporter assay, we tested a known NF-kB enhancer/promoter reporter construct. This construct utilized the same NF-kB responsive element(s) but placed them upstream an interferon beta (IFNB) minimal promoter. We tested the efficacy of this enhancer/promoter pair developed by Pomerantz et al. with the same reporters as the 'NF-kB nLuc' construct. The construct with the IFNB promoter is known as 'NF-kB IFNB.' We expect to see a similar response to stimuli in this construct as we do in the 'NF-kB nLuc' reporter. The 'NF-kB IFNB' (Figure 5B) construct was cloned via Gibson cloning using the 'nLuc-ON' backbone and the gBlock from IDT (Figure 5A). The CMV enhancer and promoter were both replaced with the NF-kB responsive elements and the IFN-beta promoter from (Pomerantz et al., 2002) (Figure 5C). The nLuc ON backbone was digested with ClaI and XbaI and the gBlock was inserted using standard Gibson cloning. The construct was verified using colony PCR, restriction digest, and sequencing. This construct contains a control for NF-kB expression, as the responsive elements and promoter have been used previously in prior literature.
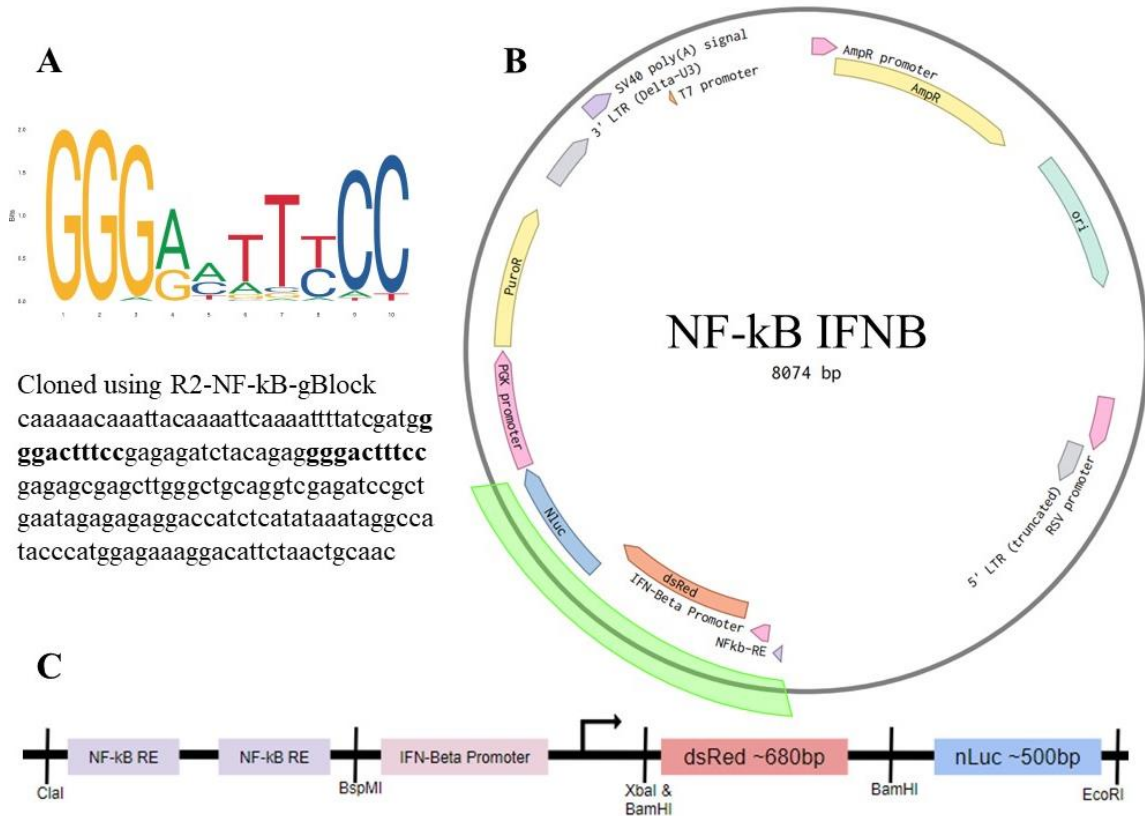
Figure 5: The NF-kB IFNB reporter. **A.** The NF-kB responsive element motif from JASPAR and the gBlock that was used to construct the NF-kB responsive region of the construct. **B**. The completed construct. **C**. detailed view of the engineered region of the construct highlighted in green.

Cloning 'CMVmin GFP' Construct

We designed a dual-fluorescence construct that would express red fluorescent protein (RFP) in the nucleus upon transfection into mammalian cells. This construct also contains the CMVmin promoter upstream a green fluorescent protein (GFP) but lacks an enhancer sequence to drive expression of GFP. This construct, called 'CMVmin GFP' serves as a control to test the efficacy of the CMVmin promoter in the dual-fluorescence construct. When transfected into mammalian cells, it is expected to produce red fluorescence in the nucleus of the cell with or without inflammatory stimulation but will not produce significant levels of green fluorescence. The dual-fluorescence control construct 'CMVmin GFP' (Figure 6A) contains a red fluorescent protein (RFP) and

12

nuclear localization protein H2B under a constitutively active hPGK promoter. It also

contains the mScarlet placeholder and CMV minimal promoter used in the previously

mentioned constructs upstream Enhanced Green Fluorescent Protein (EGFP) in the

opposite orientation as the RFP segment (Figure 6C). This construct was modified from

the pLKO-Lrp5EC-GFP-PGK-H2BRFP construct engineered by the Fuchs lab (Gonzales

et al., 2021). The H2B-RFP through EGFP segment from the Fuchs plasmid was

produced via PCR using the primers in Figure 6B and replaced the dsRed and nLuc

sequences in 'CMVmin nLuc'. This construct was verified via colony PCR, restriction

digest, and sequencing.
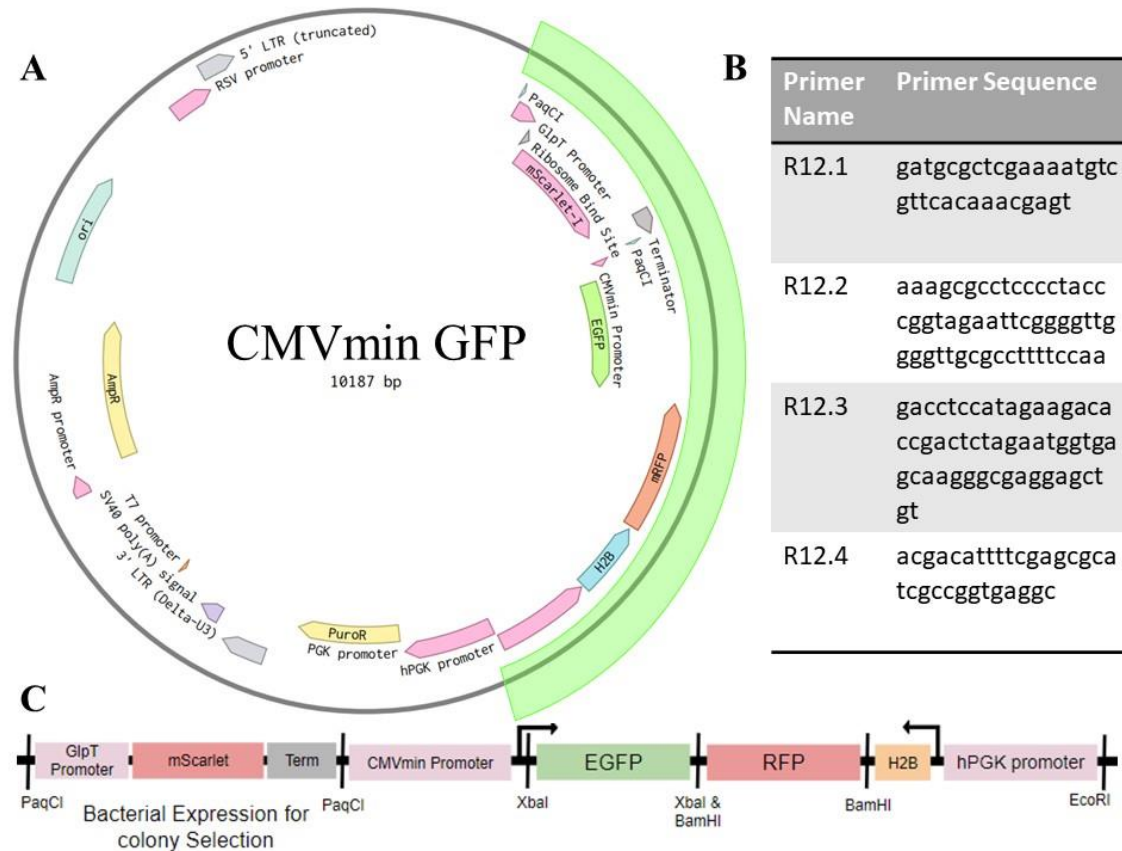
Figure 6: CMVmin GFP Reporter **A**. The completed construct **B**. The primers used to produce the dual-fluorescence region of the construct **C**. Detailed view of the engineered area (highlighted in green) that introduces dual fluorescence and the mScarlet placeholder.

Cloning 'NF-kB GFP' Construct

The dual-fluorescence reporter construct 'NF-kB-GFP' (Figure 7B) contains the same NF-kB responsive element as the 'NF-kB-nLuc' construct and was created with the same primers (Figure 7A). This reporter was engineered from the 'CMVmin GFP' reporter. The 'CMVmin GFP' construct was digested with PaqCI and the annealed oligos were cloned using standard Gibson cloning. The resulting construct was verified via colony PCR and sequencing. This construct contains the same two copies of the NF-kB responsive element upstream of the CMVmin promoter and EGFP reporter. It also contains the constitutively active RFP that will localize to the nucleus with the H2B tag.

A summary of the constructs, their important elements, and the expected effect in the mammalian cells is listed in Table 1.
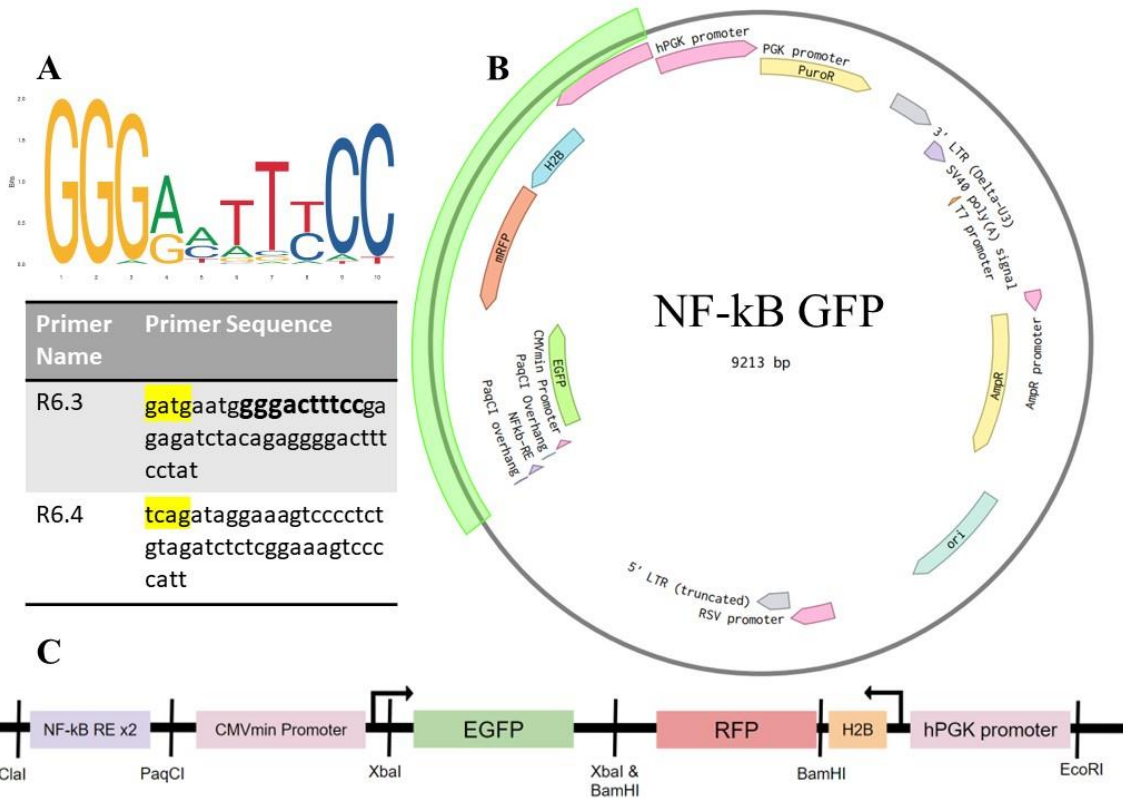
Figure 7: NF-kB GFP Reporter **A**. The NF-kB responsive element motif from JASPAR and the primers were used to construct the NF-kB responsive region. The NF-kB motif is bold, and the PaqCI overhangs are highlighted in yellow. **B**. The completed construct **C**. Detailed view of the engineered area (highlighted in green) that contains NF-kB and dual fluorescence.

Table 1

The Plasmids Comprising the Current Reporter Library

Construct Name	Important Elements	Expected Response
nLuc-ON	CMV enhancer/promoter upstream dsRed/nLuc	Constitutively active dsRed and nLuc expression throughout the cell
CMVmin nLuc	CMV minimal promoter upstream dsRed/nLuc	Little to no dsRed nor nLuc expression
NF-kB-nLuc	NF-kB responsive element upstream CMV minimal promoter and dsRed/nLuc	dsRed and nLuc expression in response to cell stimuli with NF-kB agonists PMA or LPS

NF-kB IFNB	NF-kB responsive element upstream Interferon Beta minimal promoter and dsRed/nLuc	dsRed and nLuc expression in response to cell stimuli with NF-kB agonists PMA or LPS
CMVmin GFP	hPGK enhancer/ promoter upstream RFP tagged with H2B nuclear-localizing protein. This opposite CMV minimal promoter upstream GFP	Constitutively active Red Fluorescent Protein (RFP) expression in the nucleus. No GFP expression throughout the cell
NF-kB-GFP	hPGK enhancer/ promoter upstream RFP tagged with H2B nuclear-localizing protein. This opposite NF-kB responsive element and CMV minimal promoter upstream GFP.	Constitutively active dsRed expression in the nucleus. GFP expression throughout the cell in response to stimuli with NF-kB agonists PMA or LPS

Note: A list of the current constructs comprising the reporter library. The name of the construct, the important elements for function, and the expected response are listed.

Mammalian Cell Culture

Human Embryonic Kidney (HEK) cells and Human Microglial Clone 3 (HMC3) cells were obtained from The American Type Culture Collection (ATCC) and maintained in Dulbecco's Modified Eagle Medium (DMEM) with 10% Fetal Bovine Serum (FBS) (OR 10% FB Essence) and 1% penicillin/streptomycin per the suggested maintenance conditions. All mammalian cells were stored at 37C with 5% CO_2. Cells used for these experiments did not exceed a passage number of 25. It should be noted that HEK cells are very sensitive to FBS and any changes to FBS batch or brand caused noticeable morphological differences.

Transfection, Stimuli, & Cell Collection

Cells were plated into 12-well or 24-well plates using standard media at a seeding density of 1E5 or 0.5E5, respectively, the day before transfection. HEK or HMC3 cells were transfected using L3000 lipofectamine transfection reagent (Thermo Fisher

Scientific) in the recommended 'high efficiency' ratio for a 12 well plate: 1.25ug DNA with 2.5uL P3000 reagent and 1.9uL L3000 reagent. The following day, complete media supplemented with: PMA at [2, 5, 10, or 25 ng/mL] (Hellweg et al., 2006) or LPS at [0, 100, or 500 ng/mL] (Baek et al., 2021) was added. Cells were cultured in stimuli-supplemented media for 20-24 hours. Up to four biological replicates (wells) of each reporter were tested for each experiment. Cells were collected for nanoLuciferase assay using 1x RIPA buffer and quantified via plate assay utilizing the Nano-Glo Luciferase Assay system (Promega) in a 1:1 ratio with lysed cell solution. Three technical replicates are plated from each biological replicate collected. The lysed cell solution was stored at -80 for BCA. Protein concentration of a representative number of samples from 'NF-kB nLuc' and 'NF-kB IFNB' from 1/31/2023 and 2/7/2023 were calculated using a BCA protein assay kit (Thermo Fisher Scientific).

For quantification of the 'CMVmin GFP' and 'NF-kB GFP' constructs, sterilized glass cover slides were placed in the wells and treated with 0.01% poly-l-lysine solution for ~3 hours before cells were added. After transfection and stimulation as described above, glass coverslips were collected and treated with 4% paraformaldehyde (PFA) DPBS for 15 minutes and transferred to glass slides with DAPI staining. Glass slides were incubated at room temperature, in the dark, overnight to dry and viewed on a Keyence BZ-X810 microscope the following day.

Statistics

The ROI tool from image J was used to isolate specific regions of interest of the microcopy images collected. The luminescence data from each biological replicate were

averaged to determine the mean of each sample. For the 'NF-kB nLuc' and 'NF-kB IFNB' data collected on 1/31/2023 and 2/7/2023 each data point collected for a sample was normalized to the calculated protein concentration of that sample. Luminescence values for each construct were normalized to the mean luminescence value for the construct at 0ng/mL of stimuli to better visualize fold change in luminescence. This normalization establishes the luminescence at 0ng/mL of stimulation as '1 fold' and allows for better visual identification of the change in luminescence for that construct. Data visualization and statistical analysis were performed in R and R Studio using the ggplot2 and STATS packages, respectively. A one-way ANOVA was performed with Tukey posthoc analysis utilizing a p-value < 0.05 to determine the significance of change of luminescence within a reporter construct at different stimuli concentrations. Statistical significance for p<0.05 is denoted with one star (*) and significance p< 0.01 is denoted with two stars (**).

Transcription Factors from Differential Expression

Previous enrichment analysis of HMC3 cells identified 112 genes that are upregulated in response to LPS stimulation. They utilized DESeq2 with the default parameters to identify the differentially expressed genes (Baek et al., 2021). They also utilized Gene Ontology to identify a few biological processes that are implicated by the top 50 of the 112 upregulated genes. Specifically, they employed the Database for Annotation, Visualization, and Integrated Discovery (DAVID) to calculate the Fisher's exact p-value to determine Gene Ontology Enrichment (with p<0.05 cutoff). Some of those biological processes they identified from this analysis include NF-kB response. To verify that the

activation of the NF-kB transcription factor plays a role in the regulation of these 50 genes, we performed transcription factor target analysis using the script 'find_TF_regulators.py' (Plaisier et al., 2016). The analysis compares gene lists to known and predicted transcriptional activators and calculates p-values based on Fisher's exact test. The provided p-value does not account for multiple hypothesis correction but was used as a preliminary indicator that NF-kB response was upregulated in HMC3 cells when stimulated with LPS.

RESULTS

Control Constructs in HEK Cells With PMA

First, we tested the control constructs 'nLuc ON' and 'CMVmin nLuc' in HEK cells with and without PMA stimulation. The constitutively active 'nLuc-ON' construct showed a high level of luminescence regardless of PMA concentration. This was expected because the CMV enhancer and promoter are constitutively active and should induce gene expression regardless of the stimulus. The control 'CMVmin nLuc' showed low levels of luminescence, as expected, and showed no change in luminescence at
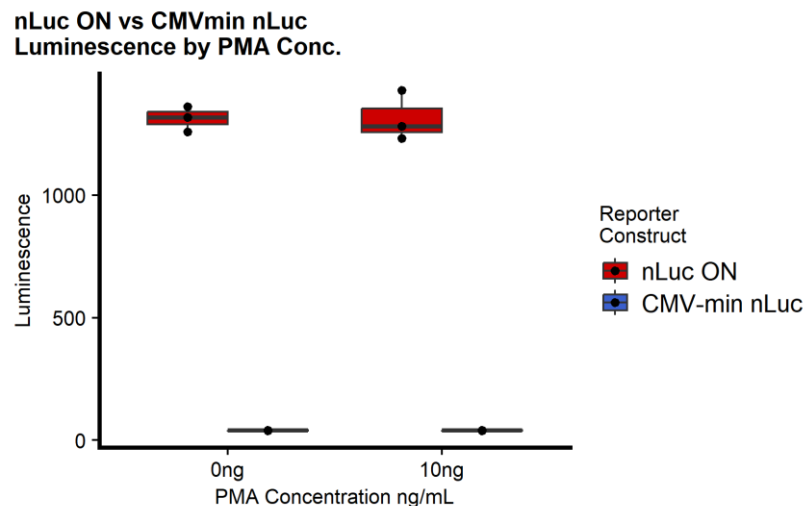

Figure 8: Control constructs 'nLuc ON' (red) and ''CMVmin nLuc' (blue) tested in HEK cells with PMA. nLuc ON shows high levels of luminescence while CMVmin nLuc shows low levels of luminescence independent of PMA concentration.

19

different PMA concentrations (Figure 8). By analyzing the constitutively active reporter and a control for the background noise of the minimal promoter, we have established a dynamic range of luminescence for reporters with this promoter. The range in luminescence varies from about 40 luminescence units as seen in 'CMVmin nLuc' to about 1500 luminescence units, as seen in 'nLuc ON' (Figure 8).

PMA Activation of NF-kB Reporter in HEK Cells With PMA

To determine the efficacy of the NF-kB Reporter, HEK cells were transfected with 'CMVmin nLuc' (the background promoter control construct) or 'NF-kB nLuc' (the experimental NF-kB dependent construct) and tested at 0ng/mL and 10ng/mL of PMA. The baseline luminescence for the 'NF-kB-nLuc' reporter at 0ng/mL of PMA stimulation was higher than the baseline luminescence for the 'CMVmin nLuc' control construct, as seen when comparing the raw luminescence values in Figure 9. This higher activity in 'NF-kB nLuc' at 0ng/mL of PMA is most likely due to background NF-kB activation that is occurring in the cells because of normal culturing conditions or transfection. The cells with the 'CMVmin nLuc' construct showed no significant change (p-value=0.98)) in luminescence at
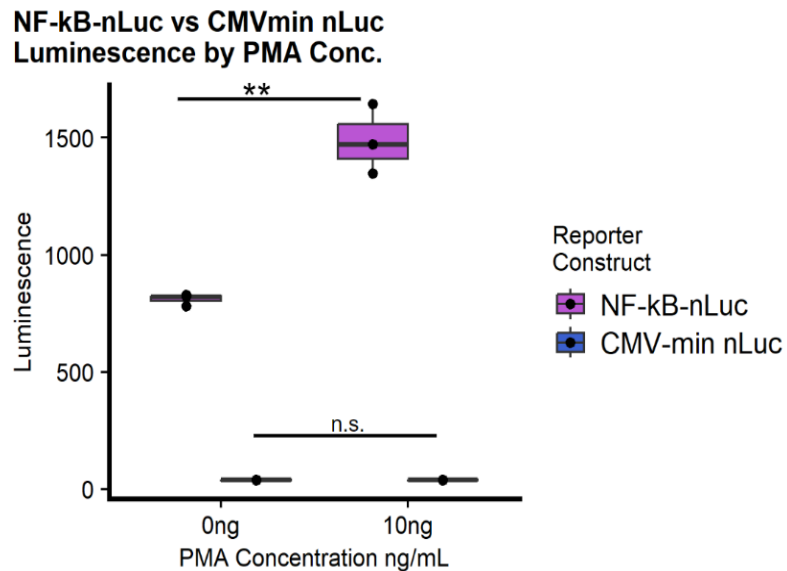

Figure 9: *Luminescence from 'NF-kB-nLuc' (purple) and 'CMVmin nLuc (blue) constructs in HEK cells compared at 0 and 10 ng/mL of PMA. Means compared with ANOVA and Tukey HSD test. (p<0.01 for **)*

20

0ng/mL vs 10ng/mL of PMA, while the cells with the 'NF-kB-nLuc' construct showed a significant increase in luminescence (p-value =0.002) (Figure 9). This indicates that the CMVmin promoter has low baseline activity and is insensitive to PMA stimulation but can be modulated by the addition of the NF-kB responsive element. Furthermore, the NF-kB enhancer allows for expression via the CMVmin promoter that is sensitive to the addition of a known NF-kB activation paradigm. We do not know, however, if the baseline expression of nLuc in either construct is due to a suboptimal arrangement of enhancer and promoter, or if there is detectable baseline activity of NF-kB without the addition of PMA.

To determine the optimal concentration of PMA needed to observe a clear response in NF-kB activation and luminescence, the 'NF-kB nLuc' reporter construct was tested in HEK cells at 0, 1, 2, 5, 10, and 25ng/mL of PMA. A statistically significant change in normalized luminescence was found between 0ng/mL of PMA and 2, 5, 10, or 25ng/mL, but not 1ng/mL. It was also clear that the highest fold change in luminescence occurred at 10ng/mL (Figure 10A). This increased response at 10ng/mL of PMA was supported by the literature (Hellweg et al., 2006). Unexpectedly, there was a drop off in fold luminescence change at 25ng/mL. While still statistically different from no PMA stimulation, there was only a 1.5x change in luminescence at 25ng/mL of PMA (Figure 10A). This may be due to the toxicity of the PMA on the HEK cells. To test this hypothesis, the luminescence was normalized to protein concentration to determine luminescence relative to cell density. For this experiment, a 50ng/mL PMA sample was included to test the potential toxicity of the PMA at higher concentrations. Without normalization, it showed a decrease in luminescence at 50ng/mL, like 25ng/mL (Figure

10B). When normalized to total protein concentration for each sample, more distinct change can be seen in luminescence/ug of total protein for all cells exposed to PMA, even at high concentrations (Figure 10C). Log2 of the fold change in luminescence was used to allow for better visualization of the changes in the luminescence in response to PMA. This demonstrates that 'NF-kB nLuc' can provide effective dose information for individual drugs, even without normalization, provided the dose is below toxic levels, but that normalization could improve clarity and decrease the signal to noise ratio.
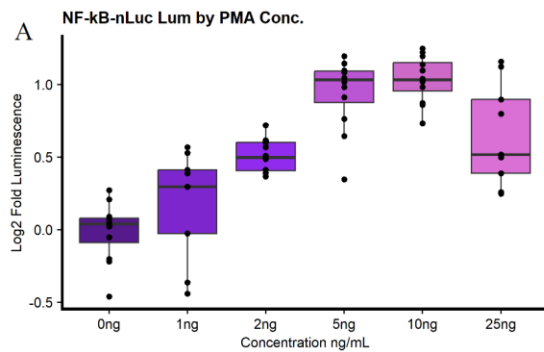
Figure 10: NF-kB-nLuc response to PMA in HEK cells log2 of luminescence fold change *A.* NF-kB nLuc response at increasing PMA concentration 0, 1, 2, 5, 10, and 25 ng/mL. *B*. Log2 fold change of NF-kB nLuc response to 0, 10, and 50 ng/mL PMA without protein normalization. *C.* Log2 fold change of NF-kB nLuc response to 0, 10, and 50ng/mL of PMA with protein normalization.
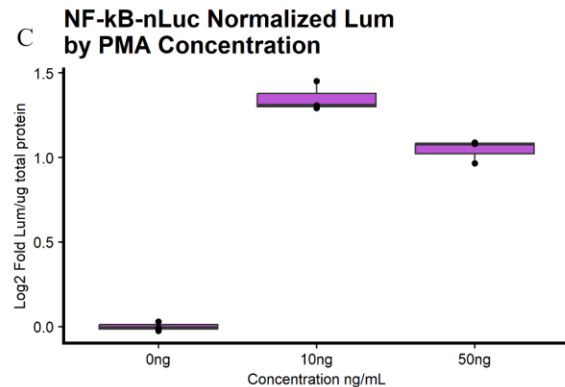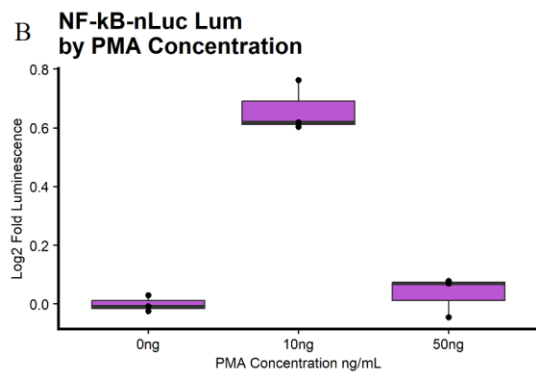
We performed the same experiment with the 'NF-kB IFNB' construct. A response similar to that of 'NF-kB nLuc' was expected, since the enhancer/promoter pair in this construct have been used as a reporter in the past (Pomerantz et al., 2002). However, the 'NF-kB IFNB' construct did not show a consistent increase in luminescence at 10ng/mL of PMA concentration, even when normalized to baseline noise at 0 ng/mL and

normalized to protein concentration for each sample, and visualized on a log2 scale of fold luminescence, which was unexpected. One trial showed an inducible 1.5-fold increase in luminescence, while another trial showed no increase at the same PMA concentration (Figure 11). This discrepancy could be due to noise introduced by activating the NF-kB pathway in the cells during the experimental process. Overgrown cells, toxicity from transfection with L3000, or general stress when plating the cells could have activated the NF-kB pathway and resulted in high levels of reporter assay activation even without PMA stimulus. Additionally, there could be a large discrepancy in transfection efficiency between one trial and the other. Low (or no) transfection efficiency would result in much lower luminescence readout from the reporter assay. Alternatively, low signal-to-noise for the 'NF-kB IFNB' reporter could also be due to the efficacy of the interferon-beta promoter, which may not be as sensitive as the CMV minimal promoter and therefore does not produce as large of a change in response after stimulation.
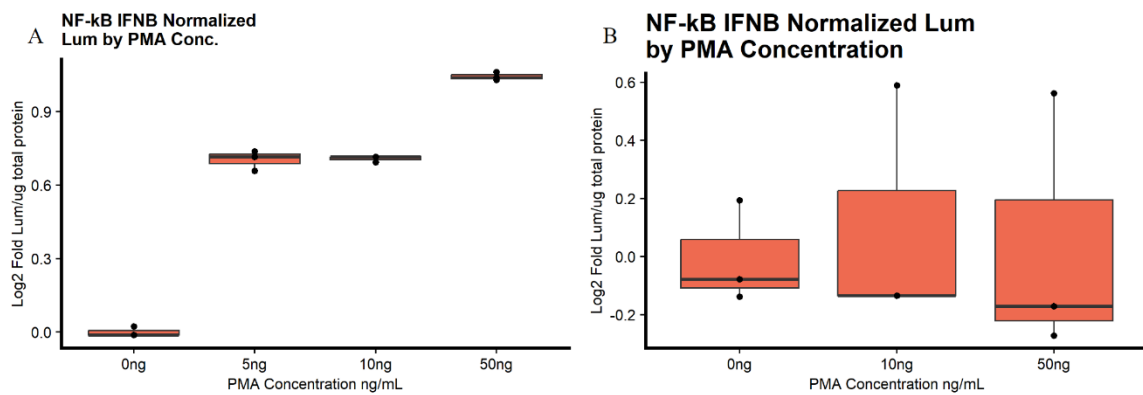
Figure 11: *NF-kB IFNB showed inconsistent NF-kB activation in HEK cells when stimulated with PMA. **A**. One trial of PMA stimulation of HEK cells with 'NF-kB IFNB' reporter, normalized to protein expression, on a log2 scale, shows a significant increase in luminescence at higher PMA concentrations. **B**. Another trial of PMA stimulation of HEK cells with the same reporter, normalized to protein expression on a log2 fold scale, shows no significant increase in luminescence at higher PMA concentrations.*

LPS Activation of NF-kB Reporter in HMC3 Cells

The goal of this project is to design a transcriptional reporter of NF-kB activity in microglia. As part of our efforts to do so, the reporter construct was translated to the microglial model cell line, HMC3. Lipopolysaccharide (LPS) activation of NF-kB is a standard assay for many immune cell types. However, in HMC3 cells some of the most well-known targets of NF-kB are not upregulated. Drawing from a study that tested the effect of LPS on HMC cells which identified 112 genes that were upregulated (Baek et al., 2021), the top 50 upregulated genes (See Appendix) were used to determine the potential transcription factors regulating the expression of those genes. These top 50 genes were analyzed by Baek et al. and identified NF-kB as a biological pathway associated with some of the genes. To confirm this, a comparison against the human TF-targets dataset showed high enrichment of genes associated with NF-kB, suggesting that LPS stimulation should cause a detectable response in this cell line. Several NF-kB transcription factor variants were identified with p-values <0.008, indicating that NF-kB binding could be occurring at the promoters of these genes (Table 2). Having verified that the NF-kB pathway can be activated in HMC3 cells by exposing them to LPS, we next tested the reporter constructs in HMC3 cells.

Table 2

NF-kB Variants Identified From TF_Targets Analysis

Transcription Factor	TF Symbol	Overlap	Overlapping Genes	P-Value
V_NFKAPPAB65_01_M00052	NFKB1	13	BIRC3 CXCL8 CXCL3 CXCL1 TNF TRAF1 CXCL10 TNFSF18	2.99E-06

			GBP4 CD69 CXCL6 TNFRSF9 CCL2	
V_NFKB_C_M 00208	NFKB1	11	TNF CXCL3 CXCL1 TRAF1 CXCL10 TNFSF18 GBP4 CD69 CXCL6 TNFRSF9 CCL2	5.42E-05
RELA_MA010 7.1	RELA	12	BIRC3 CXCL8 CXCL3 CXCL1 TNF TRAF1 CXCL10 TNFSF18 CD69 CXCL6 TNFRSF9 CCL2	1.12E-05
V_NFKB_Q6_ 01_M00774	NFKB1	14	BIRC3 TNF CXCL3 CXCL1 PTX3 TRAF1 CXCL10 TNFSF18 GBP4 CD69 CXCL6 TNFRSF9 EFNA1 CCL2	4.28E-06
NF-kappaB_MA00 61.1	NFKB1	14	BIRC3 TNF CXCL3 CXCL1 TRAF1 CXCL10 TNFSF18 GBP4 CD69 CXCL6 TNFRSF9 CCL2 TNFAIP2 CXCL11	2.53E-07
V_P50P50_Q3_ M01223	NFKB1	11	TNF PTX3 TRAF1 BCL2A1 CXCL10 TNFSF18 ACTA1 GBP4 VCAM1 TNFRSF9 CXCL6	3.31E-05
V_P50RELAP6 5_Q5_01_M01 224	NFKB1	15	TNF CXCL3 C1QTNF1 CXCL1 TRAF1 CXCL10 IL1B TNFSF18 CD69 VCAM1 CXCL6 TNFRSF9 CCL2 TNFAIP2 CXCL11	3.15E-07
NFKB2_NFAT _DBD_dimeric _13_1	NFKB2	5	CXCL3 CXCL1 TRAF1 TNFSF18 CXCL6	0.00251 7
NFKB1_NFAT _DBD_dimeric _13_1	NFKB1	4	CXCL3 PTX3 TNFSF18 TRAF1	0.00800 8
V_CREL_01_ M00053	REL	13	BIRC3 CXCL8 CXCL3 CXCL1 TNF TRAF1 BCL2A1 TNFSF18 CD69 CXCL6 TNFRSF9 CCL20 CCL2	1.07E-06
V_NFKB_Q6_ M00194	NFKB1	12	CXCL8 TNF TRAF1 CXCL10 TNFSF18 GBP4 SIDT1 CD69 CXCL6 TNFRSF9 CCL2 CSF2	1.25E-05
V_NFKAPPAB 50_01_M00051	NFKB1	3	BIRC3 TRAF1 CD69	0.11947 9

			BIRC3 CXCL8 CXCL3 CXCL1 TNF TRAF1 BCL2A1 TNFSF18 CD69 CXCL6 TNFRSF9 CCL20	
REL_MA0101. 1	REL	13	CCL2	1.07E-06
V_NFKAPPAB _01_M00054	NFKB1	14	BIRC3 TNF CXCL3 CXCL1 TRAF1 CXCL10 TNFSF18 GBP4 CD69 CXCL6 TNFRSF9 CCL2 TNFAIP2 CXCL11	2.53E-07
NFKB1_MA01 05.1	NFKB1	6	CXCL3 CXCL1 TRAF1 TNFSF18 TNFRSF9 CXCL6	0.00110 2

Note: NF-kB variants identified from TF_Targets analysis. The transcription factor name, number of overlapping genes, list of genes, and p-value from Fisher's exact test are listed above.

HMC3 cells were transfected with the NF-kB Responsive reporter and stimulated with LPS at 0 or 100 ng/mL of LPS. of NF-kB in HMC3 cells. While the constitutively active 'nLuc-ON' reporter showed consistent luminescence as expected, 'NF-kB-nLuc' reporter activity was inconsistent across experiments and required normalization during analysis to show differences in nLuc expression. One trial showed a significant increase in response to LPS stimulation, while another trial showed no significant increase in NF-kB activation (Figure 12). This discrepancy in luminescence output from the 'NF-kB nLuc' reporter may be due to inconsistent transfection efficiency of the construct into the cells. It could also be due to elevated levels of baseline NF-kB expression due to mishandling of the cells causing additional stress and activation of the inflammatory pathway. This discrepancy could also be due to a lack of normalization to total protein concentration or number of transfected cells. These samples were not normalized to protein expression to see if non-normalized data would provide enough information about NF-kB induce luminescence. To better understand the response to LPS activation, another engineering iteration of the reporter construct is necessary to introduce a means

26

to determine the transfection efficiency of the construct before stimulation and allow for
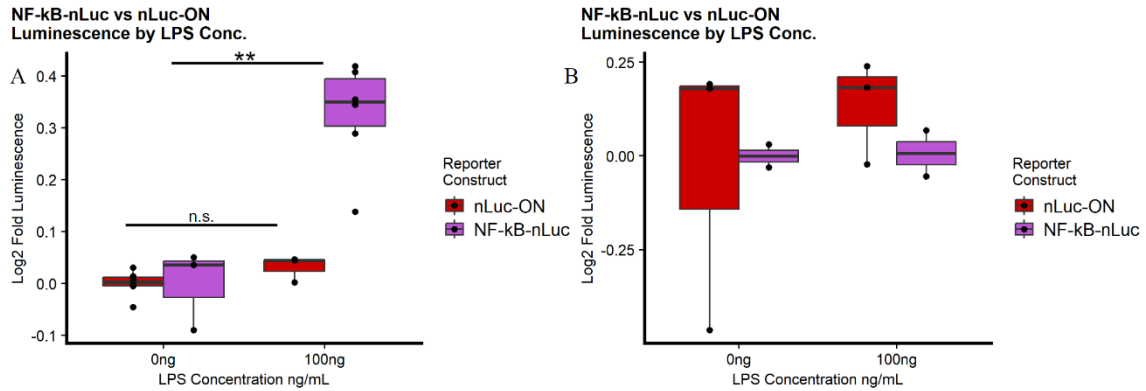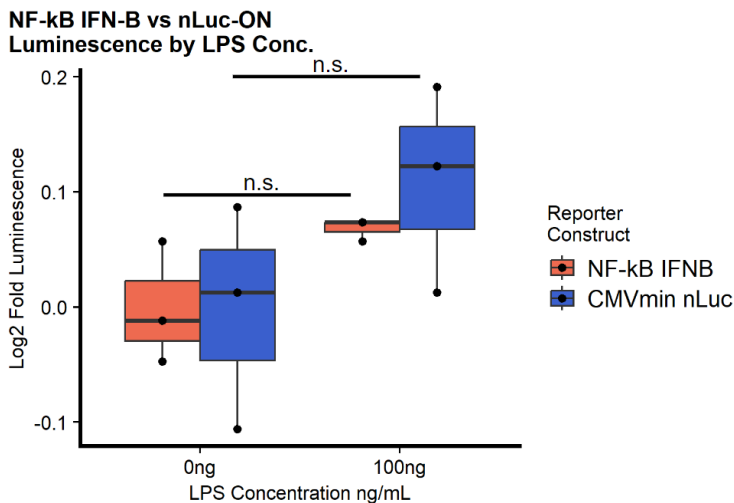
normalization.

*Figure 12: NF-kB-nLuc activation compared to nLuc-ON expression in HMC3 cells exposed to LPS, normalized to background noise at 0ng/mL. **A.** One trial of LPS stimulation of NF-kB-nLuc activation shows a 1.3-fold significant increase in luminescence with 100 ng/mL of LPS. **B.** Another trial of LPS stimulation of NF-kB-nLuc activation showed no significant increase in luminescence.*

Additionally, there was no significant change in the luminescence in the control

'NF-kB IFNB' reporter. This response more closely resembled that of the 'CMVmin

nLuc' construct, neither of which showed a significant change at 100ng/mL of LPS

(Figure 13). This discrepancy from trial to trial may be due to an error in the

experimental protocol or an inconsistency with the HMC3 cell line. These experiments

demonstrate how our transcriptional reporter yields larger signal changes than previous

designs and how one assay can correlate with transcriptomic data.

Figure 13: NF-kB IFNB (orange) vs nLuc-on (blue) luminescence in HMC3 cells exposed to 0 or 100 ng/mL of LPS, normalized to noise from 0ng/mL.

PMA Activation of Dual Fluorescence Reporter in HEK Cells

We further iterated on our transcriptional reporter architecture using microscopy studies. Single fluorescence can present noise across individual cells, depending on transfection levels or expression due to cell viability. We added a second fluorescent reporter, targeted to the nucleus for normalization of general expression levels. The control construct, 'CMVmin GFP' was again tested in HEK cells stimulated with 10ng/mL PMA. It showed RFP expression, but no GFP expression (Figure 14). This construct was expected to produce high levels of red fluorescence localized to the nucleus, and little to no green fluorescence when stimulated with PMA. As seen in Figure 14A, there was little to no green fluorescence. While there were many cells (Figure 14B), there was low transfection efficiency as indicated by the low red fluorescence levels in the nuclei (Figure 14C). The dual fluorescent reporter, 'NF-kb GFP,' was also tested in HEK cells stimulated with 10ng/mL of PMA. This reporter was expected to produce red fluorescent protein localized to the nucleus and express green fluorescent protein when exposed to PMA at 10ng/mL. In comparison to the 'CMVmin GFP' construct, increased green fluorescence co-localized to the transfected red fluorescent cells was seen in some transfected cells (Figure 14D). However, there was also very low transfection efficiency as seen by the low number of red fluorescent nuclei (Figure 15C). The red fluorescent protein serves as a positive control for transfection efficiency. This observable low transfection efficiency may account for the discrepancies in NF-kB activation seen in prior iterations of the reporter constructs.
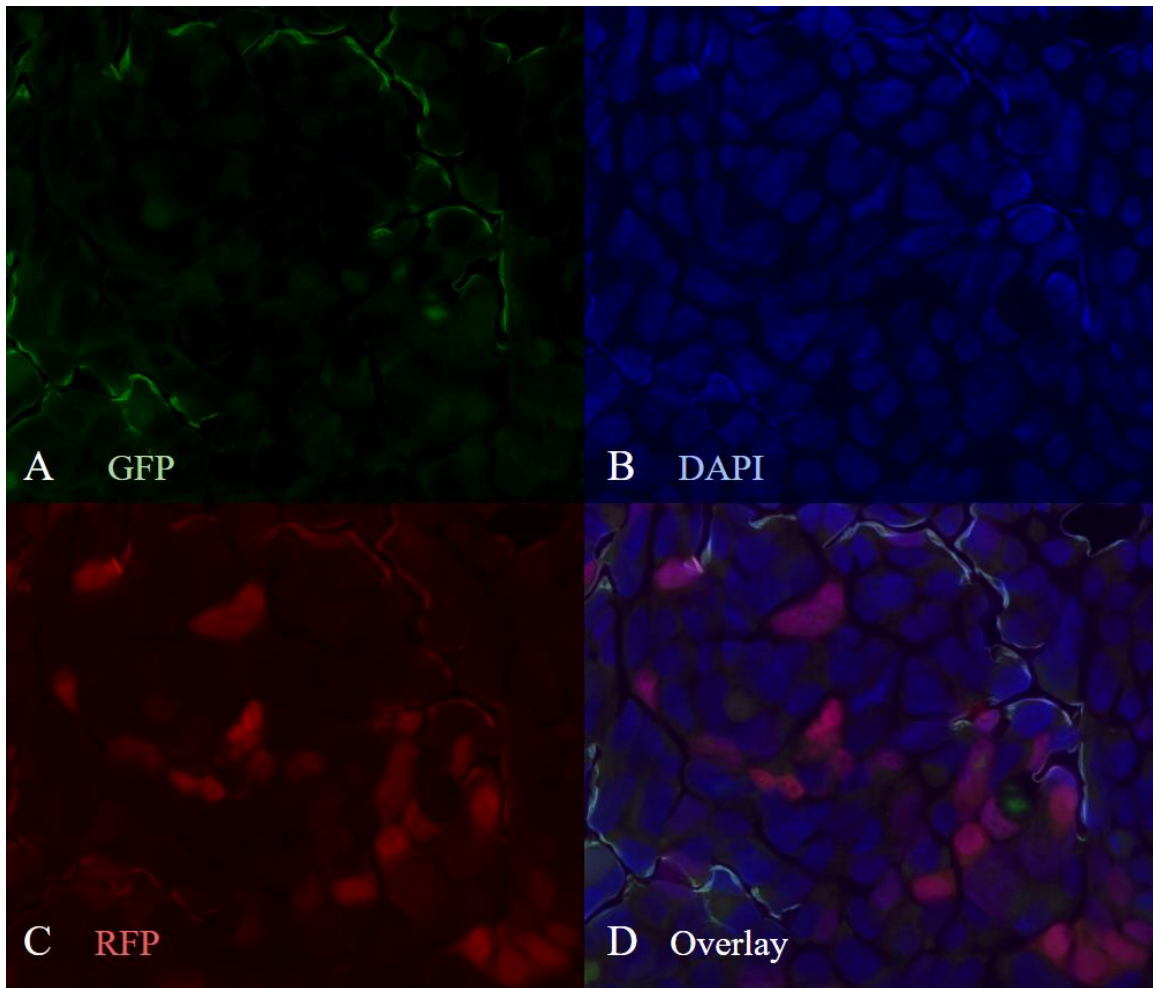
Figure 14*: HEK cells transfected with 'CMVmin GFP' Stimulated with 10 ng/mL PMA under 40X magnification **A**: NF-kB responsive EGFP expression **B**: DAPI staining of the nuclei of HEK cells. **C**: RFP protein tagged with H2B localizing to cell nucleus D: Overlay of A, B, and C shows little to no EGFP expression in transfected cells after stimulation with PMA.*
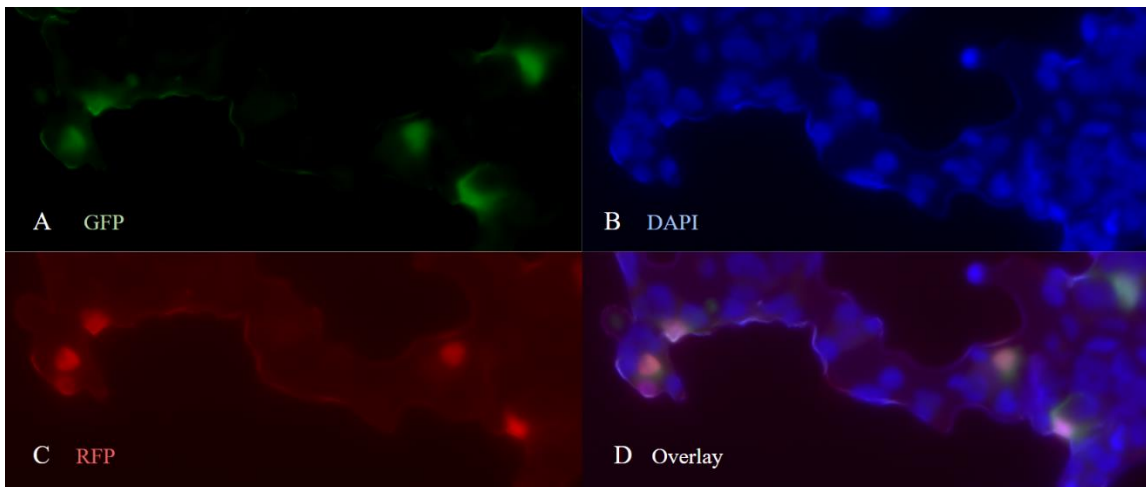
Figure 15: *HEK cells transfected with 'NF-kB GFP Reporter' Stimulated with 10ng/mL PMA under 40X magnification* ***A***: *NF-kB responsive EGFP expression* ***B***: *DAPI staining of the nuclei of HEK cells.* ***C***: *RFP protein tagged with H2B localizing to cell nucleus* ***D***: *Overlay of A, B, and C shows co-localization of RFP and GFP in some cells, as seen by lighter areas.*

CONCLUSIONS AND FUTURE DIRECTIONS

We have engineered and produced a library of reporter constructs to measure NF-kB response in mammalian cells. Preliminary data shows that the CMVmin promoter utilized in this construct does not exhibit significant background activity, even at high levels of PMA or LPS stimulation. However, when paired with the NF-kB responsive element, the NF-kB enhancer CMVmin promoter pair can produce an NF-kB dependent response showing an increase in luminescence in HEK cells. This shows a higher signal-to-noise ratio than previous NF-kB architectures that utilize a different promoter ('NF-kB IFNB'). However, there is some inconsistency between different experimental trials of the 'NF-kB IFNB' construct. This issue with inconsistent NF-kB response occurs with the 'NF-kB IFNB' construct in response to PMA in HEK cells, and with the 'NF-kB nLuc' construct in response to LPS in HMC3 cells. This may be due to low transfection efficiency in some trials, which could result in an insignificant change in luminescence,

due to the low number of cells that were transfected and are therefore capable of producing the luminescent protein. To combat this issue, we engineered a dual-fluorescent protein that contains a constitutively active red fluorescent protein opposite the NF-kB dependent reporter, green fluorescent protein. This construct (and the associated CMVmin control construct) showed very low transfection rates but did show some co-localization of GFP and RFP in response to 10ng/mL of PMA in HEK cells transfected with the 'NF-kB GFP' reporter. This preliminary data indicates that this NF-kB CMVmin enhancer/promoter pair could serve as a reliable reporter assay for NF-kB activation in mammalian cells.

Future work should be conducted to increase the transfection efficiency of all the reporter constructs. Then, the luminescence or fluorescence should be normalized to the total number of transfected cells, rather than the total protein expression from the wells to provide a more accurate analysis of change in luminescence per transfected cell. For the 'NF-kB GFP' and the 'CMVmin GFP' dual reporter constructs, future work should focus on quantitatively comparing the red fluorescence to the green fluorescence within a single cell. This will allow for a more accurate analysis of the change in luminescence by introducing a positive control within each cell to compare the intensity NF-kB response. Fluorescence can be measured with microscopy or with flow cytometry, which would allow for higher throughput single cell comparisons. Improving the accuracy of the reporter assay enables us to study the inflammatory states that can be induced in the cells. This library of reporter constructs should be made available to other researchers to build on and use in their research. Alternative NF-kB responsive element sequences could be tested to determine the optimal sequence to study inflammatory activity in cells, and the

effect of the number of repeated enhancer elements could also be tested. This library could also be translated to different microglial cell types, such as iPSC-derived or primary microglia, to determine if this assay can accurately represent NF-kB activation in a more biologically accurate microglial model.

Expanding the library of reporter constructs could aid in drug screening and development for neurodegenerative diseases like Parkinson's and Alzheimer's. The standard drug development process relies heavily on identifying specific mechanisms of disease with therapies specifically designed to block or counteract them (*Drug Development Basics*, n.d.). For an untargeted drug, however, direct counteractive mechanisms in one cell type can cause severe side effects in neighboring cells. An alternative approach to counteract cellular pathology is to induce cell-specific responses to new therapies. The cell-specific change in functional state can be assayed by the broad transcriptional changes, morphological changes, or by assessing cell state (Nowacek et al., 2009). Our assay could be used to generate a preliminary profile of the changes in transcriptional programs that by monitoring changes in transcription factor activity in response to novel stimuli. For example, this reporter assay platform could be used to screen for drugs that target the inflammatory pathways of microglia. It could also be translated into other neuronal cell lines to study the potential transcriptional pathways that may be activated as a side effect of treatment with a new drug. By expanding our knowledge of the transcriptional response of neuroimmune cells to new drugs we can hopefully improve the preliminary drug screening and development process for every neurodegenerative disease with an inflammatory component.

32

REFERENCES

Baek, M., Yoo, E., Choi, H. I., An, G. Y., Chai, J. C., Lee, Y. S., Jung, K. H., & Chai, Y. G. (2021). The BET inhibitor attenuates the inflammatory response and cell migration in human microglial HMC3 cell line. *Scientific Reports*, *11*(1), Article 1. https://doi.org/10.1038/s41598-021-87828-1

Brasier, A. R., & Ron, D. (1992). Luciferase reporter gene assay in mammalian cells. *Methods in Enzymology*, *216*, 386–397. https://doi.org/10.1016/0076-6879(92)16036-J

DiSabato, D., Quan, N., & Godbout, J. P. (2016). Neuroinflammation: The Devil is in the Details. *Journal of Neurochemistry*, *139*(Suppl 2), 136–153. https://doi.org/10.1111/jnc.13607

Drug development basics. (n.d.). Retrieved February 13, 2023, from https://www.baybridgebio.com/blog/drug_dev_process.html

Engler, C., Kandzia, R., & Marillonnet, S. (2008). A One Pot, One Step, Precision Cloning Method with High Throughput Capability. *PLoS ONE*, *3*(11), e3647. https://doi.org/10.1371/journal.pone.0003647

Gibson, D. G., Young, L., Chuang, R.-Y., Venter, J. C., Hutchison, C. A., & Smith, H. O. (2009). Enzymatic assembly of DNA molecules up to several hundred kilobases. *Nature Methods*, *6*(5), Article 5. https://doi.org/10.1038/nmeth.1318

Hammond, T. R., Marsh, S. E., & Stevens, B. (2019). Immune Signaling in Neurodegeneration. *Immunity*, *50*(4), 955–974. https://doi.org/10.1016/j.immuni.2019.03.016

Hellweg, C. E., Arenz, A., Bogner, S., Schmitz, C., & Baumstark-Khan, C. (2006). Activation of Nuclear Factor κB by Different Agents. *Annals of the New York Academy of Sciences*, *1091*(1), 191–204. https://doi.org/10.1196/annals.1378.066

Lier, J., Streit, W. J., & Bechmann, I. (2021). Beyond Activation: Characterizing Microglial Functional Phenotypes. *Cells*, *10*(9), 2236. https://doi.org/10.3390/cells10092236

Lim, P. S., Sutton, C. R., & Rao, S. (2015). Protein kinase C in the immune system: From signalling to chromatin regulation. *Immunology*, *146*(4), 508–522. https://doi.org/10.1111/imm.12510

Lively, S., & Schlichter, L. C. (2018). Microglia Responses to Pro-inflammatory Stimuli (LPS, IFNγ+TNFα) and Reprogramming by Resolving Cytokines (IL-4, IL-10). *Frontiers in Cellular Neuroscience*, *12*. https://www.frontiersin.org/articles/10.3389/fncel.2018.00215

Neurodegenerative Diseases. (2022, June 9). National Institute of Environmental Health Sciences. https://www.niehs.nih.gov/research/supported/health/neurodegenerative/index.cfm

Paolicelli, R. C., Sierra, A., Stevens, B., Tremblay, M.-E., Aguzzi, A., Ajami, B., Amit, I., Audinat, E., Bechmann, I., Bennett, M., Bennett, F., Bessis, A., Biber, K., Bilbo, S., Blurton-Jones, M., Boddeke, E., Brites, D., Brône, B., Brown, G. C., … Wyss-Coray, T. (2022). Microglia states and nomenclature: A field at its crossroads. *Neuron*, *110*(21), 3458–3483. https://doi.org/10.1016/j.neuron.2022.10.020

Pomerantz, J. L., Denny, E. M., & Baltimore, D. (2002). CARD11 mediates factor-specific activation of NF-kappaB by the T cell receptor complex. *The EMBO Journal*, *21*(19), 5184–5194. https://doi.org/10.1093/emboj/cdf505

Salter, M. W., & Stevens, B. (2017). Microglia emerge as central players in brain disease. *Nature Medicine*, *23*(9), Article 9. https://doi.org/10.1038/nm.4397

Shao, F., Wang, X., Wu, H., Wu, Q., & Zhang, J. (2022). Microglia and Neuroinflammation: Crucial Pathological Mechanisms in Traumatic Brain Injury-Induced Neurodegeneration. *Frontiers in Aging Neuroscience*, *14*, 825086. https://doi.org/10.3389/fnagi.2022.825086

Vallabhapurapu, S., & Karin, M. (2009). Regulation and Function of NF-κB Transcription Factors in the Immune System. *Annual Review of Immunology*, *27*(1), 693–733. https://doi.org/10.1146/annurev.immunol.021908.132641

Verstrepen, L., Bekaert, T., Chau, T.-L., Tavernier, J., Chariot, A., & Beyaert, R. (2008). TLR-4, IL-1R and TNF-R signaling to NF-kB: variations on a common theme. *Cellular and Molecular Life Sciences*, 2964–2978. https://doi.org/10.1007/s00018-008-8064-8

Yang, W., Hamilton, J. L., Kopil, C., Beck, J. C., Tanner, C. M., Albin, R. L., Ray Dorsey, E., Dahodwala, N., Cintina, I., Hogan, P., & Thompson, T. (2020). Current and projected future economic burden of Parkinson's disease in the U.S. *NPJ Parkinson's Disease*, *6*, 15. https://doi.org/10.1038/s41531-020-0117-1

Yu, H., Lin, L., Zhang, Z., Zhang, H., & Hu, H. (2020). Targeting NF-κB pathway for the therapy of diseases: Mechanism and clinical study. *Signal Transduction and Targeted Therapy*, *5*(1), Article 1. https://doi.org/10.1038/s41392-020-00312-6

Zhang, L., Wei, X., Wang, Z., Liu, P., Hou, Y., Xu, Y., Su, H., Koci, M. D., Yin, H., & Zhang, C. (2023). NF-κB activation enhances STING signaling by altering microtubule-mediated STING trafficking. *Cell Reports*, *42*(3), 112185. https://doi.org/10.1016/j.celrep.2023.112185

APPENDIX

A   TRANSCRIPTION FACTOR REGULATORS – TOP 50 GENE LIST FROM

BAEK ET AL.

Table 3

Top 50 genes upregulated in HMC3 cells with LPS. From Baek et al.

Gene Symbol	log$_2$FoldChange
CCL20	6.5
CSF3	5.6
MMP3	5.5
LTB	5.0
CXCL10	5.0
TNF	4.7
CXCL8	4.6
TNFSF18	4.6
CD69	4.5
MIR146A	4.4
CCL2	4.4
MMP12	4.3
FSCN2	4.3
ZNF197-AS1	4.2
CXCL11	4.1
MIR593	4.0
ZBP1	4.0
CSF2	4.0
ZNF385C	3.9
ACTA1	3.8
UBE2Q2L	3.8
CETN4P	3.7
CXCL6	3.6
CXCL1	3.5

LMO2	3.5
TNFAIP2	3.5
SIDT1	3.4
GBP5	3.4
C16orf71	3.4
GBP1P1	3.3
IL1B	3.2
TNFRSF9	3.2
CXCL3	3.2
IFNL1	3.2
GBP2	3.1
C3AR1	3.1
C1QTNF1	3.0
PHACTR1	3.0
NEURL3	2.9
VCAM1	2.9
IFNB1	2.9
TRAF1	2.8
PCDH17	2.8
GBP4	2.7
EFNA1	2.7
PTX3	2.7
BIRC3	2.6
MMP13	2.6
SERPINB2	2.6
BCL2A1	2.5

Note: These are the top 50 genes upregulated in HMC3 cells in response to LPS at
100ng/mL. The log2FoldChange indicates how differentially expressed the gene is

compared to unstimulated HMC3 cells. This analysis was completed by (Baek et al., 2021). This is the list of genes we used to determine if NF-kB transcription factors would be upregulated in LPS-stimulated HMC3 cells.